

Interaction of two flapping filaments in a flowing soap film

Luoding Zhu^{a)} and Charles S. Peskin

Courant Institute of Mathematical Sciences, New York University, 251 Mercer Street, New York, New York 10012

(Received 16 September 2002; accepted 23 April 2003; published 5 June 2003)

Using the immersed boundary method, we have simulated the motion of two flexible filaments in a flowing soap film, which was experimentally studied by Zhang *et al.* [Nature (London) **408**, 835 (2000)]. We found numerically two distinct modes of sustained oscillation of the two filaments: parallel flapping and mirror-image clapping, depending on the separation distance between the two filaments. Our simulation results agree with that of the experiment at least qualitatively, even though the Reynolds number of the flowing soap film in our simulation is about two orders of magnitude lower than that of the experiment. © 2003 American Institute of Physics.

[DOI: 10.1063/1.1582476]

I. INTRODUCTION

Fluid-structure interaction¹ is important in biomechanics. Improved understanding of biological fluid-structure interaction could lead to engineering applications that exploit the design principles of Nature. Even the passive problem of a flapping filament in a flowing soap film (the two-dimensional analog of a flag flapping in the wind) has much to teach us about biological swimming² and about fluid-structure interaction in general.

This paper is motivated by the experiments of Zhang *et al.*³ on the dynamics of flexible filaments in a flowing soap film. Figure 1 shows the setup of the laboratory experiment. At the top of the apparatus, there is a reservoir of soapy water, below which a stopcock is attached to control the rate of discharge from the reservoir. Two thin nylon wires diverge at the nozzle, run downwards diverging until they meet the upper supporting threads marked “T” in the figure, and then proceed vertically downwards forming the parallel sides of the flow channel in which the experiment is to be performed. The vertical course of the wires ends well below the region of interest at the lower supporting threads (again marked “T”), below which the wires converge carrying the flowing soap solution into a collecting chamber. With the stopcock open, the soapy water will fall out of the reservoir under the influence of gravity, thus forming a thin layer of soap film bounded by the two edge wires. The falling soap film soon reaches its terminal velocity determined by the balance of gravity and air resistance. Two thin flexible filaments are placed in the flowing soap film with their upper ends fixed at a height where the film has already reached its terminal velocity. The two fixed ends are symmetrically placed with respect to the vertical midline of the apparatus, in the same horizontal line, and separated by a distance that may be controlled by the experimentalist. This distance turns out to be an important parameter of the experiment.

Without the filaments, the flowing soap film flow may be approximately treated as a two-dimensional channel flow, which has a simple analytical solution, even in the presence of air resistance. (For more information on the hydrodynamics of soap films, see Refs. 4–7. For more information on filament dynamics in fluids, see Refs. 8, 9.) However, after the introduction of the filaments, because of the interaction between the flexible filaments and the flowing soap film, the motion of the system becomes both complicated and interesting: the filaments move at the local fluid velocity of the soap film, the two-dimensional velocity field of which they simultaneously influence through the forces that they apply to the surrounding fluid. These forces are influenced by the elasticity and inertia of the filaments. They have the effect of generating vorticity, some of which is washed down along the sides of the filaments by the flowing soap film. At the free ends of the filaments, vortices are shed and are subsequently advected by the flow, and dissipated by the combined effect of viscous diffusion and air resistance.

The experiment parameters are listed in Table I (column 2). One of the interesting findings of the experiment is that, when the distance d between the fixed ends of the filaments is small enough ($d/L < 0.21 \pm 0.04$, where L is the filament length), the two filaments execute in-phase parallel flapping, but when that same distance is large enough ($d/L > 0.21 \pm 0.04$), they switch to an antiphase clapping motion. For details of the experimental findings, see Zhang.³

We have previously simulated the flapping motion of a *single* flexible filament in a flowing soap film by the immersed boundary (IB) method, see Zhu,¹⁰ Zhu and Peskin.¹¹ Here, we report our IB simulation of *two* interacting flexible filaments in a flowing soap film. Although our methodology is unchanged, consideration of the two-filament system introduces a rich repertoire of possible behavior. This is because the two filaments may influence each other through the flowing soap film that contains both. As a result of this influence, their motion may become synchronized in more than one way, as described above.

^{a)}Present address: Department of Computer Science, University of California at Santa Barbara, Santa Barbara, CA 93106. Telephone: (805) 893-5728; electronic mail: zhuld@cs.ucsb.edu

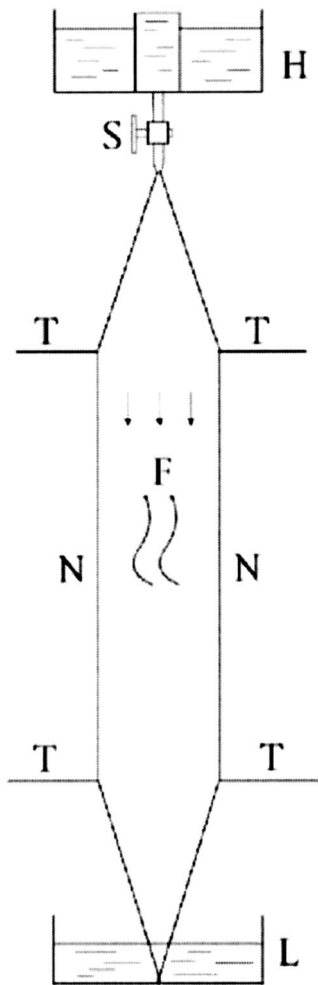


FIG. 1. The laboratory experimental setup (courtesy of the experimentalist, Zhang *et al.*, Ref. 3). H: soapy water container, S: stopcock, N: nylon wire, F: filament, L: receiver, T: supporting thread.

II. MATHEMATICAL FORMULATION AND NUMERICAL METHOD

As shown in Table I, the filament diameter ($150 \mu\text{m}$) is much greater than the film thickness ($3\text{--}4 \mu\text{m}$), so the actual physical situation involves a three-dimensional filament moving in an almost two-dimensional film (see Fig. 2). The main hypotheses made for the filament-in-film problem are:

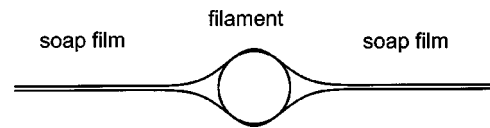


FIG. 2. Cross section of the film-filament system.

- (1) The filament is a one-dimensional curve with negligible volume and with mass uniformly distributed on this one-dimensional curve, which is totally immersed in the soap film. The curve behaves like a linear elastic material line which can be stretched, compressed, and bent, and which resists these deformations by elastic forces.
- (2) The flowing soap film is an incompressible, viscous, Newtonian fluid membrane with zero thickness which cannot be stretched or compressed. The surface tension between the film and the filament has a negligible effect on the filament motion, despite its significance in forming a bulge of fluid around the filament and thereby increasing the effective filament mass. The flow within the soap film is a two-dimensional plane laminar flow governed by the incompressible Navier–Stokes equations. (Chomaz,¹³ Chomaz and Cathalau¹⁴ have shown that the flowing soap film can be described by the 2D incompressible Navier–Stokes equations if the typical film flow speed is smaller than the Marangoni elastic wave speed and if the initial film thickness variation and total soap concentration are small. We believe that these conditions hold in the experiments of Zhang *et al.*³ to which our computational results are compared.)
- (3) The magnitude of air resistance (drag force per unit area) is proportional to the local film speed, and the proportionality factor is a constant in space and time. The direction of the air resistance is opposite to that of the flow at each point.
- (4) The effective mass of a filament is twice the measured mass of that filament wet by soapy water. The extra mass comes from a bulge in the film that forms around the filament as a result of surface tension. The factor of 2 is a rough estimate of this effect, based on the observed geometry of the bulge in the film.
- (5) The filament-film system is not sensitive to the film length or to the outflow condition at the bottom of the film, provided the film is long enough in comparison to the filament length.

TABLE I. Parameters of the laboratory experiment and simulation.

	Experiment value	Simulation value
Film inflow velocity	200–300 cm/s	220 cm/s
Film dynamic viscosity	1.2×10^{-5} g/s	1.2×10^{-3} g/s
Film density	3×10^{-4} g/cm ²	3×10^{-4} g/cm ²
Film thickness	$(3\text{--}4) \times 10^{-4}$ cm	0.0
Filament diameter	0.015 cm	0.0
Filament length	2–6 cm	3.6 cm
Filament density	2×10^{-4} g/cm	4×10^{-4} g/cm
Filament rigidity	0.1 erg·cm	0.1 erg·cm
Gravitational acceleration	980 cm/s ²	980 cm/s ²
Width of the film	8.5 cm	8.5 cm
Length of the film	120 cm	17 cm

With these assumptions, a mathematical formulation of our problem that includes filament mass and elasticity, gravity, air resistance, and the two wires that bound the flowing soap film, may be written as a system of integrodifferential equations that can be solved numerically by the IB method. Currently, there exist several versions of the IB method.^{10–12,15–22} The version we employ here is the one used in Refs. 10, 11. Its novel feature is the ability to handle filament mass in the manner described below. The incompressible viscous Navier–Stokes equations, which are used in our formulation to describe the motion of the whole film-

filament system are discretized into a fixed uniform two-dimensional Eulerian mesh, whereas the filament equations are discretized into moving Lagrangian one-dimensional arrays of points (one array for each filament) whose nodes do not necessarily coincide with the fixed Eulerian mesh points of the fluid computation. The delta function approximation that mediates the interaction between the filament and the soap film is used not only to interpolate the fluid velocity and to apply force to the fluid, but also to handle the mass of the filament, which is represented in our calculation as a delta function layer of fluid mass density supported along each of the immersed filaments. Because of this nonuniform mass density, we use a multigrid (seven-grid V-cycle) method^{23–25} for solving the discretized fluid equations. For details, see Refs. 10, 11.

III. SIMULATION RESULTS

The parameters used in our simulation are shown in Table I (column 3). The dynamical viscosity μ is larger (and therefore the Reynolds number is smaller) by two orders of magnitude in our simulations than in the corresponding experiments. The mass of each filament is twice that measured by weighing each filament saturated with soapy water. As discussed above, the extra mass is intended to model the mass of the bulge in the film that forms around each filament as a result of surface tension.

The vertical length of the domain in our computation is shorter than the experimental soap film, but it does not appear that the length of the film is an important parameter, provided it is long enough not to interfere with filament motion. The elastic stretching stiffness coefficient in our simulation is chosen such that the filament experiences almost no stretch ($<0.5\%$ of filament length). The filament separation distance d is taken as $0.1L$, $0.3L$, and $0.6L$, where L is the length of each filament. All other parameters besides the Reynolds number, the filament mass, and the length of the film are the same as those in the experiment.

We employ two different techniques in this paper to visualize the simulation results: the instantaneous position of fluid markers and the contours of vorticity. In the following figures where these visualizations are used, the left panels show the instantaneous positions of fluid markers, and the right panels show vorticity contours. The fluid markers were generated in bursts intermittently, like hydrogen bubbles generated by pulses of electrical current to provide flow visualization in a physical experiment. In both (left and right) panels of each figure, flow is from top to bottom (driven by gravity, falling against air resistance) at an inflow velocity that is equal to the film terminal velocity. The initial configuration chosen for the two filaments is a pair of in-phase parallel sine waves separated by a distance d , with amplitude 25% of the length of the two filaments. The multigrid computation within each time step is performed on a series of grids with resolution 256×512 on the finest level. The multigrid Navier–Stokes solver is terminated in each time step when the L_2 norm of the relative residual falls below 10^{-6} . We have found that a stricter criterion makes little difference in the overall result of the computation. The simulation is run

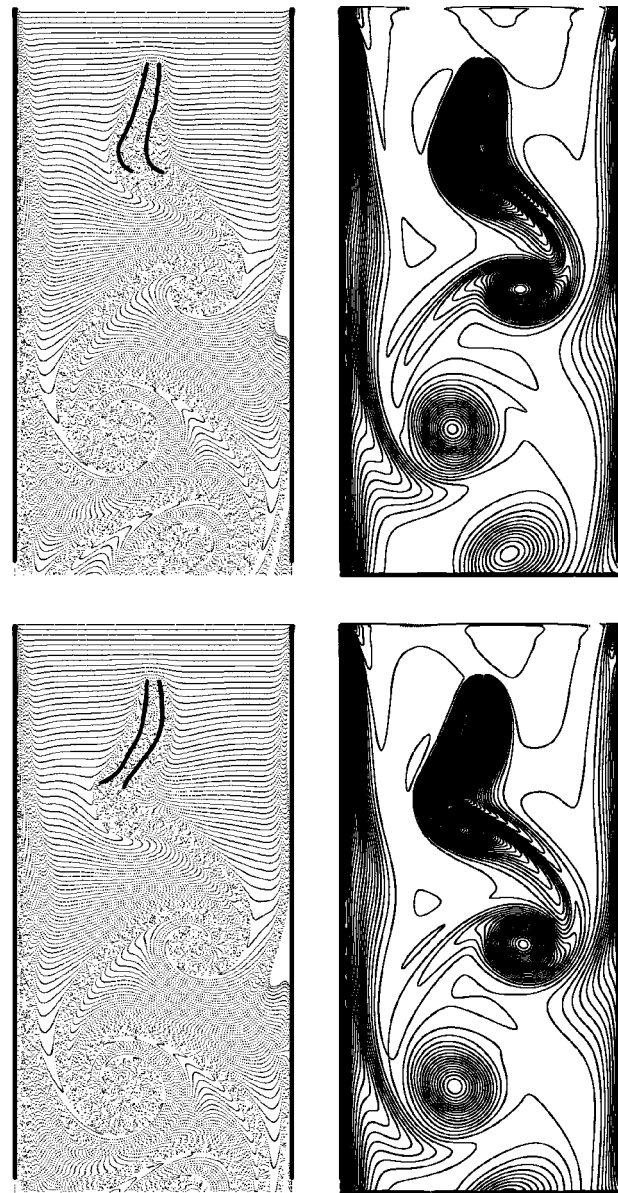


FIG. 3. The in-phase flapping of two filaments in a flowing soap film. Here and in all similar figures, the left panels show particle positions, the particles having been introduced in pulses at equal time intervals and equally spaced in x along the inflow boundary. The particles that comprise the two filaments are also shown. The right panels show vorticity contours at the corresponding times. The filament length is 3.6 cm. The distance between the two fixed ends of the filaments is $0.1 \times$ filament length. Time = 0.173 s in the upper pair of frames, and time = 0.178 s in the lower pair.

up to 0.2 second, which is enough to cover 6–8 cycles of the observed spontaneous oscillations of the filaments.

Figures 3 and 4 show simulation results of two filaments separated by a distance $d/L = 0.1$. Although not shown here, one can see from an animation of the simulation results that the two filaments, starting from the initial configuration and, following approximately one oscillation, quickly settle into a sinuous, parallel, in-phase flapping. One may argue that this is not surprising, since the initial condition is already one in which the two filaments are parallel. It is not always the case, however, that the symmetry of the sustained motion is the same as that of the initial condition, as we shall see later. In each stroke, vortices are shed away from the two free ends

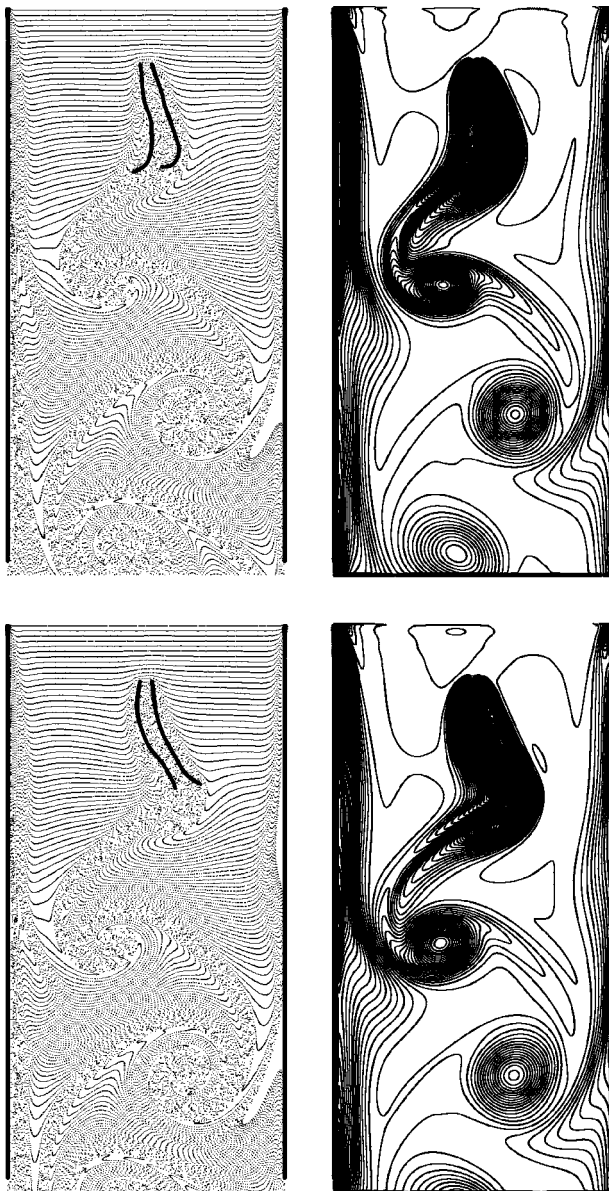


FIG. 4. Continued from Fig. 3; time=0.189 s in the upper pair of frames, and time=0.1945 s in the lower pair.

with alternating signs, the leftward stroke generating counterclockwise vortices, and the rightward stroke generating clockwise vortices. When these vortices are carried away by the flowing soap film, a mushroomlike structure develops, and a vortex street forms downstream. The stem of the mushroom structure is approximately perpendicular to the flow direction. (See left panels of Figs. 3 and 4.) The flapping frequency is about 29 Hz. The parallel flapping is self-sustained and periodic in time. Figure 5 shows the x coordinate of the position of the free end of each of the two filaments as a function of time. The dotted lines are the x coordinates of the positions of the two tethered ends, for comparison.

When the filament separation distance is increased to $d/L=0.3$, while all the other parameters are kept the same, one can see from an animation that the parallel configuration of the initial condition is not maintained as time evolves.

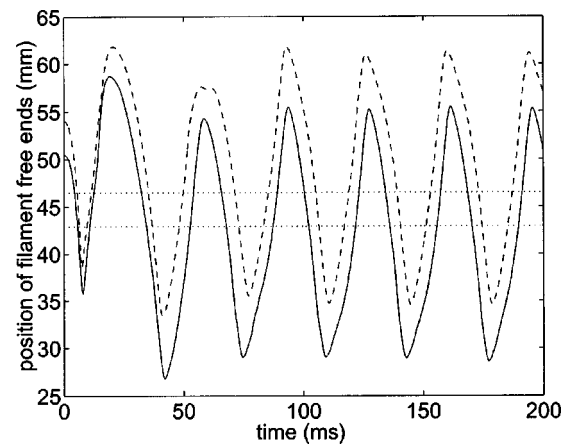


FIG. 5. The x coordinates of the two filament free ends as functions of time. The two filaments are separated by a distance d such that $d/L=0.1$, where L is filament length. The filaments execute in-phase flapping. The solid line refers to the filament on the left and the dashed line refers to the filament on the right. The dotted lines are the x coordinates of the two tethered ends.

Instead, after a short adjustment period, the filaments settle into their stable antiphase flapping state: a clapping motion that is symmetrical with respect to the flow midline. This is a striking result, since the parallel initial condition would seem to bias the filaments away from the sustained anti-parallel motion that they eventually find. When the two free ends of the filaments reach the outer limits of the motion, vortices of opposite sign (the left filament producing counterclockwise and right filament producing clockwise vortices) are shed from the free ends of the filaments. These vortex pairs are carried downstream by the flowing soap film, and they deform the fluid between them which rolls up into a mushroom shaped structure as revealed by the fluid markers. The vortices shed from the free ends when the filaments clap together are carried away and form the stem of the next mushroom. Unlike the scenario in parallel flapping, the shaft of the mushroom structure is nearly aligned with the flow direction of the film, so that each mushroom looks like a falling parachute (see left panels of Figs. 6 and 7). The simulation results are visualized in Figs. 6 and 7 at four different instants. The clapping frequency is about 41 Hz, which is approximately 41% higher than the flapping frequency of the in-phase case. (In Zhang's experiment the corresponding increase is about 35%.) Clapping is periodic in time and self-sustaining. Figure 8 shows a plot of the x coordinates of the two free end position as functions of time.

When the filament separation distance is increased still further, e.g., $d/L=0.6$, the coupling between the two filaments becomes very weak and each of them executes periodic sinuous flapping motion almost independently, resembling a *single* filament in a flowing soap film, see Refs. 10, 11. When the wakes behind the two filaments are advected downstream by the flowing fluid, they get entangled with each other and the interaction of the two wakes makes the downstream flow look more chaotic and the mushroom-like structure is no longer evident, see Fig. 9.

We also performed simulations on two interacting *massless* filaments, by setting the parameter of filament mass equal to zero in each of the three cases reported above, while

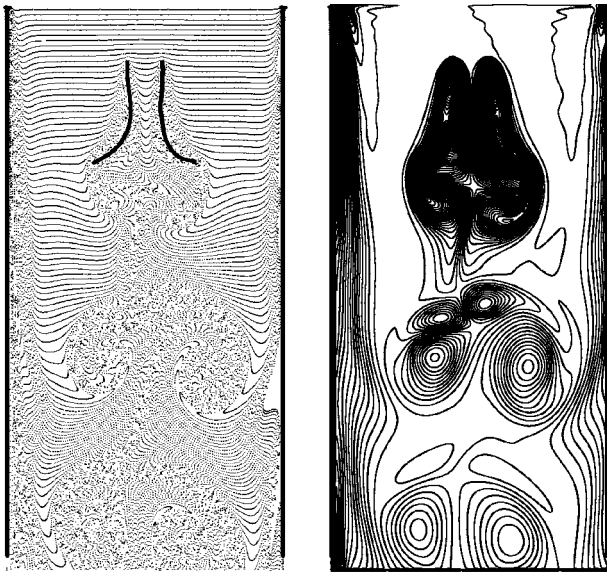


FIG. 6. The clapping motions of two filaments in a flowing soap film. The filament length is 3.6 cm and the fixed ends of the two filaments are separated by $0.3 \times$ filament length. Time=0.18 s in the upper pair of frames, and time=0.185 s in the lower pair.

keeping all the rest of the parameters unchanged. We found in each case that both filaments return to their straight parallel line state aligned with the flow direction following a short period of damped oscillations. As in Refs. 10, 11, this shows the significant role that the filament mass plays in the dynamics of flapping.

In the experiment, the transition from in-phase behavior to antiphase behavior was found to occur at a separation distance d_c given by $d_c/L = 0.21 \pm 0.04$. This is consistent with our result, which is that d_c/L lies somewhere between 0.1 and 0.3. We have not yet tried to define the critical distance more precisely.

IV. SUMMARY AND CONCLUSION

This work extends our earlier simulation study^{10,11} of a single flapping filament in a flowing soap film to the case of

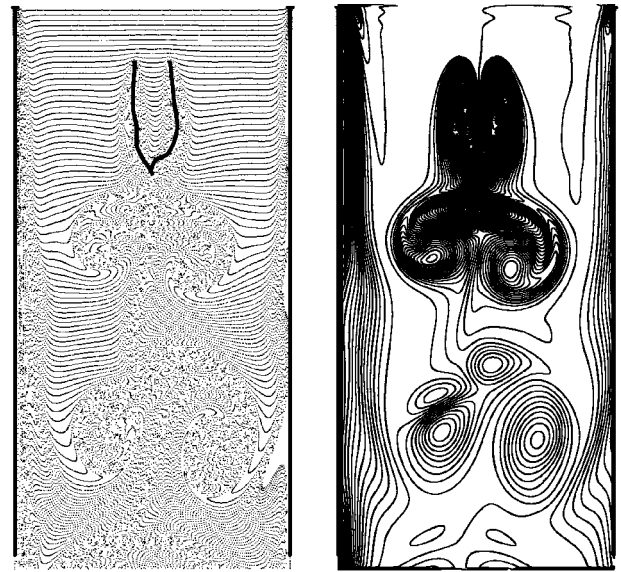


FIG. 7. Continuation of Fig. 6 at two later times: time=0.19 s in the upper pair of frames, and time=0.195 s in the lower pair.

two interacting filaments. In both studies, a version of the immersed boundary method that allows for filament mass was used. The earlier study showed that filament mass was essential for sustained flapping, and that result is confirmed here in the case of two interacting filaments.

With two interacting filaments side by side in a flowing soap film, we have found two distinct modes of sustained synchronized flapping. Which mode occurs depends on the dimensionless parameter d/L , where d is the separation distance between the two filaments and L is their length. For $d/L = 0.1$ we find parallel (in-phase) flapping, and for $d/L = 0.3$ we find an antiparallel or clapping motion in which the two filaments oscillate in antiphase. The latter result is particularly striking because our standard initial condition in these studies involves two *parallel* sinusoidal filaments. The clapping motion has a substantially higher frequency of oscillation than the parallel flapping motion, and the down-

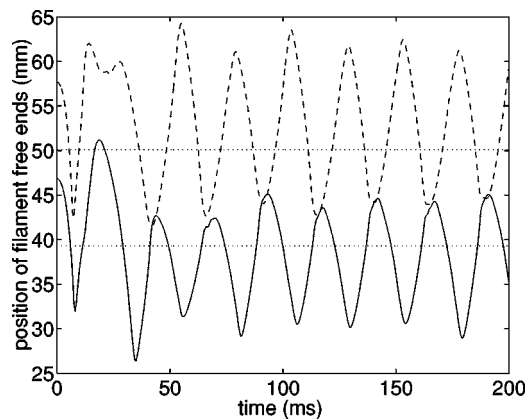


FIG. 8. The x coordinates of the two filament free ends as a function of time. The two filaments are separated by a distance d such that $d/L=0.3$, where L is filament length, which is 3.6 cm. The inflow speed is 220 cm/s. Even though the two filaments start in phase with each other, they spontaneously switch to antiphase oscillation after about one cycle, and remain in antiphase thereafter. The solid line refers to the filament on the left and the dashed line refers to the filament on the right. The dotted lines are the x coordinates of the two tethered ends.

stream flow pattern also looks considerably different in the two cases.

When the two filaments are even further apart ($d/L=0.6$), we find that their motions become uncoupled and the downstream flow pattern becomes somewhat chaotic. This deserves further study, since the chaotic motion may be an indication of a transition between two different stable oscillatory modes.

All of these results are in agreement with the experiments³ that inspired the present study. Although most of the parameters of the simulation are the same as those in the experiment, one notable difference is that the Reynolds number of the simulation (200) is lower than that of the experiment (20 000) by a factor of 100. This suggests that the Reynolds number, once it is sufficiently high, is not a very important parameter for the flapping filament problem. The dynamical system comprised of one or more flexible filaments in a flowing soap film has a rich mathematical structure that includes at least the phenomena of bistability (for a single filament, see Refs. 3, 10, 11), in-phase synchronization, and antiphase synchronization. We have shown that a computational model based on the immersed boundary method captures the full range of these behaviors.

In addition to the Reynolds number and the dimensionless separation distance, the filament-film system has several other nondimensional parameters, e.g., the filament dimensionless mass, see Refs. 10, 11. The influences of dimensionless parameters other than the dimensionless filament separation distance d/L on the qualitative behavior of the two-filament system have not been studied in the present paper. It is quite possible that the critical values of d/L (i.e., those values at which a transition from one qualitative behavior to another occurs) may be influenced by the other dimensionless parameters of the problem. This is a good subject for future research.

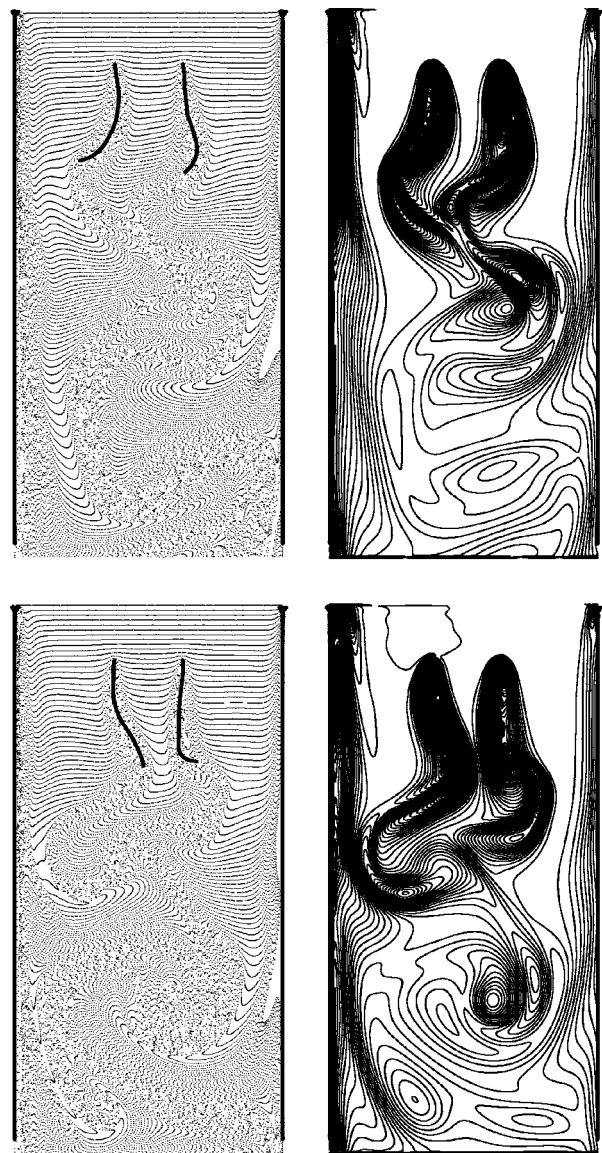


FIG. 9. The motion of the two-filament-film system when the inter-filament distance $d=0.6 \times$ filament length. The inflow is 220 cm/s, and filament length is 3.6 cm. Time=0.1600 s in the upper pair of frames, and time=0.1965 s in the lower pair. The flapping motions of the two filaments are nearly independent.

ACKNOWLEDGMENTS

The authors are indebted to the National Science Foundation (USA) for support of this work under KDI research Grant No. DMS-9980069. We also thank Jun Zhang for many discussions of the experiment, Peter Schmid for discussion of the multigrid method, Michael Shelley and Stephen Childress for helpful discussions of the flapping-filament problem, and David McQueen for help in using computers.

¹M. P. Paidoussis, *Fluid-Structure Interaction*, Vol. 1 (Academic, San Diego, 1998).

²G. Huber, "Swimming in Flatsea," *Nature (London)* **408**, 777 (2000).

³J. Zhang, S. Childress, A. Libchaber, and M. Shelley, "Flexible filaments in a flowing soap film as a model for one-dimensional flags in a two-dimensional wind," *Nature (London)* **408**, 835 (2000).

- ⁴Y. Couder, J. M. Chomaz, and M. Rabaud, "On the hydrodynamics of soap films," *Physica D* **37**, 384 (1989).
- ⁵M. Gharib and P. Derango, "A liquid film (soap film) tunnel to study two-dimensional laminar and turbulent shear flows," *Physica D* **37**, 406 (1989).
- ⁶H. Kellay, X.-I. Wu, and W. I. Goldburg, "Experiments with turbulent soap films," *Phys. Rev. Lett.* **74**, 3975 (1995).
- ⁷M. A. Rutgers, X.-I. Wu, R. Bhagavatula, A. A. Peterson, and W. I. Goldburg, "Two-dimensional velocity profiles and laminar boundary layers in flowing soap films," *Phys. Fluids* **8**, 2847 (1996).
- ⁸M. J. Shelley and T. Ueda, "The Stokesian hydrodynamics of flexing, stretching filaments," *Physica D* **146**, 221 (2000).
- ⁹L. E. Becker and M. J. Shelley, "Instability of elastic filaments in shear flow yields first-normal-stress differences," *Phys. Rev. Lett.* **87**, 198301 (2001).
- ¹⁰L. Zhu, "Simulation of a flapping flexible filament in a flowing soap film by the immersed boundary method," Ph.D. thesis, Courant Institute, New York University (2001).
- ¹¹L. Zhu and C. S. Peskin, "Simulation of a flapping flexible filament in a flowing soap film by the immersed boundary method," *J. Comput. Phys.* **179**, 452 (2002).
- ¹²M. Rivers and X. L. Wu, "External dissipation in driven two-dimensional turbulence," *Phys. Rev. Lett.* **85**, 976 (2000).
- ¹³J. M. Chomaz, "The dynamics of a viscous soap film with soluble surfactant," *J. Fluid Mech.* **442**, 387 (2001).
- ¹⁴J. M. Chomaz and B. Cathalau, "Soap films as a classic fluids," *Phys. Rev. A* **41**, 2243 (1990).
- ¹⁵C. S. Peskin, "The immersed boundary method," *Acta Numerica* **11**, 479 (2002).
- ¹⁶C. S. Peskin, "Flow patterns around heart valves: A numerical method," *J. Comput. Phys.* **25**, 220 (1977).
- ¹⁷C. S. Peskin and D. M. McQueen, "Fluid dynamics of the heart and its valves," in *Case Studies in Mathematical Modeling: Ecology, Physiology, and Cell Biology*, edited by H. G. Othmer, F. R. Adler, M. A. Lewis, and J. C. Dallon (Prentice-Hall, Englewood Cliffs, NJ, 1996), p. 309.
- ¹⁸C. S. Peskin and D. M. McQueen, "Computational biofluid dynamics," *Contemp. Math.* **141**, 161 (1993).
- ¹⁹C. S. Peskin and B. F. Printz, "Improved volume conservation in the computation of flows with immersed elastic boundaries," *J. Comput. Phys.* **105**, 33 (1993).
- ²⁰M. C. Lai and C. S. Peskin, "An immersed boundary method with formal second order accuracy and reduced numerical viscosity," *J. Comput. Phys.* **160**, 705 (2000).
- ²¹M. C. Lai, "Simulations of the flow past an array of circular cylinders as a test of the immersed boundary method," Ph.D. thesis, Courant Institute, New York University (1998).
- ²²D. M. McQueen and C. S. Peskin, "Heart simulation by an immersed boundary method with formal second order accuracy and reduced numerical viscosity," in *Mechanics for a New Millennium: Proceedings of the ICTAM 2000*, edited by H. Aref and J. W. Phillips (Kluwer Academic, Dordrecht, The Netherlands, 2000).
- ²³W. L. Briggs, V. E. Henson, and S. F. McCormick, *A Multigrid Tutorial*, 2nd ed. (SIAM, Philadelphia, 2000).
- ²⁴W. H. Press, S. A. Teukolsky, W. T. Vetterling, and B. P. Flannery, *Numerical Recipes in Fortran: The Art of Scientific Computing*, 2nd ed. (Cambridge University Press, Cambridge, 1992), p. 862.
- ²⁵A. Brandt, *Multigrid Techniques: Guide with Application to Fluid Dynamics*, GMD-Studien Nr. 85, Gesellschaft für Mathematik und Datenverarbeitung (St. Augustin, Bonn, 1984).

Physics of Fluids is copyrighted by the American Institute of Physics (AIP).
Redistribution of journal material is subject to the AIP online journal license and/or AIP
copyright. For more information, see <http://ojps.aip.org/phf/phfcr.jsp>
Copyright of Physics of Fluids is the property of American Institute of Physics and its
content may not be copied or emailed to multiple sites or posted to a listserv without
the copyright holder's express written permission. However, users may print,
download, or email articles for individual use.